THE ASTROPHYSICAL JOURNAL, 565:1239–1250, 2002 February 1

EMPIRICAL BOUNDS FOR THE IONIZING FLUXES OF WOLF-RAYET STARS

DAVID R. LAW,[1] KATHLEEN DEGIOIA-EASTWOOD, AND KEVIN L. MOORE[2]
Department of Physics and Astronomy, Northern Arizona University, P.O. Box 6010, Flagstaff, AZ 86011-6010; drlaw@virginia.edu, kathy.eastwood@nau.edu, klmoore@socrates.berkeley.edu
Received 2001 August 8; accepted 2001 October 8

ABSTRACT

Hα photometry and spectroscopic data have been obtained for 10 Wolf-Rayet nebulae, representing a wide variety of WN spectral types. We use these data to constrain the ionizing flux of the exciting Wolf-Rayet star, calculating lower bounds for the Lyman continuum flux (Q_0) and for the He^0- and He^+-ionizing fluxes (Q_1 and Q_2). We find that Q_0 appears independent of WN spectral type, and lower bound estimates tend to cluster around 48 dex. Finally, we discuss the effects of potential shock excitation and density bounding on these nebulae and compare our results to recent models. Our results are consistent with the predictions of line-blanketed ISA-wind models and nonblanketed CMFGEN models but are consistent with only some of the line-blanketed CMFGEN models.

Subject headings: H II regions — stars: fundamental parameters — stars: Wolf-Rayet

1. INTRODUCTION

Readily identifiable in any spectroscopic survey by their pronounced emission lines, Wolf-Rayet (WR) stars present somewhat of an enigma. Current theory holds that WR stars are highly evolved descendants of massive OB stars (Conti 2000) and exhibit extremely high temperatures and significant mass loss in strong stellar winds. In part because of the extended outer layers of the stellar atmosphere and extensive mass loss by the stellar winds, the spectral energy distribution (SED) of the star deviates substantially from a simple blackbody. This deviation can create significant complications for many galactic studies, such as population synthesis models and calculations of star formation rates, which rely upon accurate knowledge of the SED contribution of component star types.

While these WR stars cannot be studied in the extreme UV directly as a result of absorption by the interstellar medium (ISM), the surrounding nebulae can provide valuable insight. These nebulae are composed of interstellar gas enriched by ejecta from the evolving OB star and can be both photoionized and shock ionized by the WR star. While photoionization can also occur from other stars, the H-ionizing flux from the lowest luminosity WR star is comparable to that from an O3 V star (assuming that the O star radiates as a blackbody), so effects on the WR nebula from stray later type O stars should not be significant. If the nebula is primarily photoionized, by observing Hα emission we can work backward (e.g., Osterbrock 1974) to obtain the Lyman continuum flux required to produce the observed nebular luminosity. Using the relative strengths of spectral emission lines, it is possible to estimate the relative luminosity of each nebula at all other observed emission wavelengths as well, from which we can deduce lower bounds for the He^0- and He^+-ionizing fluxes. We use this modified Zanstra method to estimate the UV SED of 10 Galactic WR nebulae, selected from the catalog of van der Hucht (2001).

While similar studies have been pursued previously by a number of authors, actual ionizing fluxes have generally not been calculated. Instead, the Zanstra method has historically been employed to calculate the stellar surface temperature using a blackbody model. However, because of the extended atmosphere of the star, optical depth varies substantially with wavelength, and the WR star departs significantly from a standard blackbody, therefore making Zanstra temperature estimates ambiguous.

Lately, efforts have focused primarily on calculating an effective stellar surface temperature by constructing increasingly complex stellar models to reconstruct the observed stellar emission. These stellar atmosphere models are capable of estimating expected ionizing fluxes, and it is these parameters which we attempt to empirically constrain. For a more thorough introduction to WR stars, atmospheres, and nebulae the reader is advised to consult Conti (2000), Hillier (1987), and Smith (1995), respectively.

2. OBSERVATIONS

2.1. *Spectroscopy*

Long-slit spectroscopy of WR nebulae was obtained by K. D.-E. at Kitt Peak National Observatory (KPNO) using the 2.1 m telescope with the GoldCam F3KC CCD. Spectroscopy covered 4000–6900 Å (resolution 5 Å) with a slit length of 5′.2 and a width of 3″.1. The slit was positioned to measure bright knots in the structure of each nebula pictured in Miller & Chu (1993). As spectroscopy was obtained before photometry, spectral data for WR 141 were taken with the slit positioned on nebulosity that we later conclude may not be primarily photoionized by the WR star (further explained in § 2.2).

Standard bias subtractions and flat-field divisions were performed before extracting one-dimensional spectra, and IRAF routines were used to eliminate cosmic-ray hits and CCD chip defects located primarily at 5354 and 5365 Å. Spectra were then flux calibrated using observations of the spectrophotometric standard stars of Massey et al. (1988). The emission line ratios Hα/Hβ were then compared to the value of 2.87 expected under case B recombination theory (Osterbrock 1974), and extinction was calculated assuming the canonical value of $R_V = 3.1$ and using the standard extinction model of Savage & Mathis (1979). Spectra were then dereddened using standard IRAF routines.

[1] Visiting REU Researcher. Current address: P.O. Box 3818, Department of Astronomy, University of Virginia, Charlottesville, VA 22903-0818.

[2] Visiting REU Researcher. Current address: Department of Physics, University of California, Berkeley, Berkeley, CA 94720-7300.

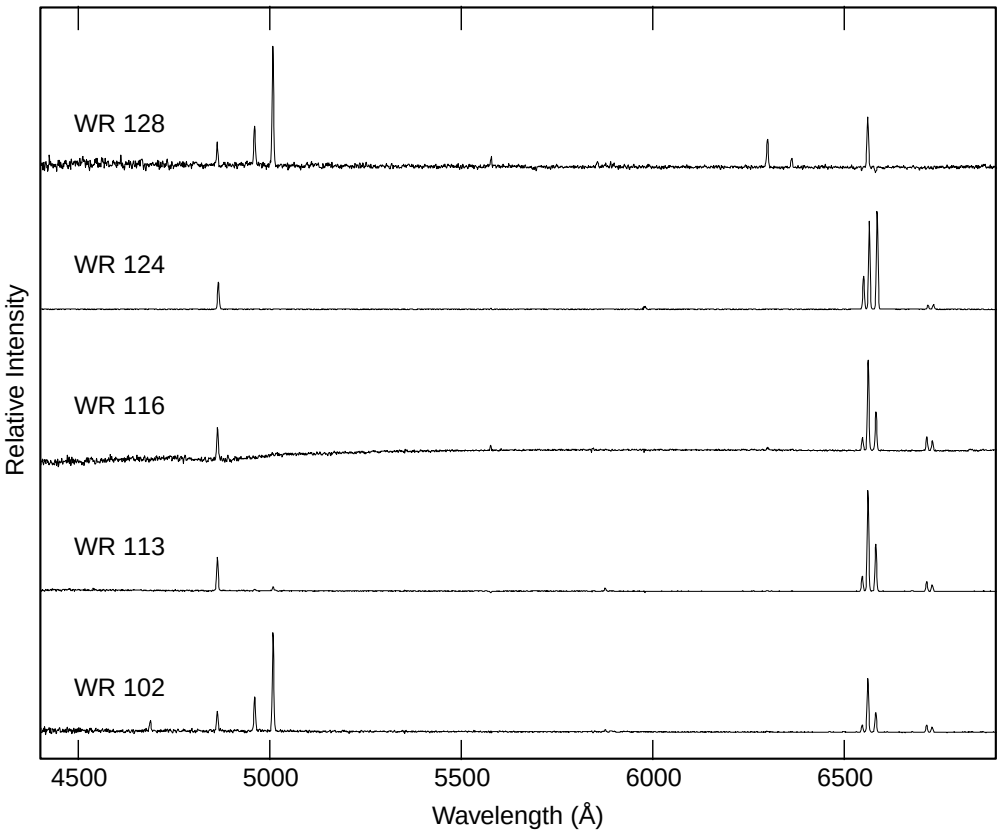

FIG. 1.—Dereddened spectra of WR nebulae, listed by the number of the central WR star

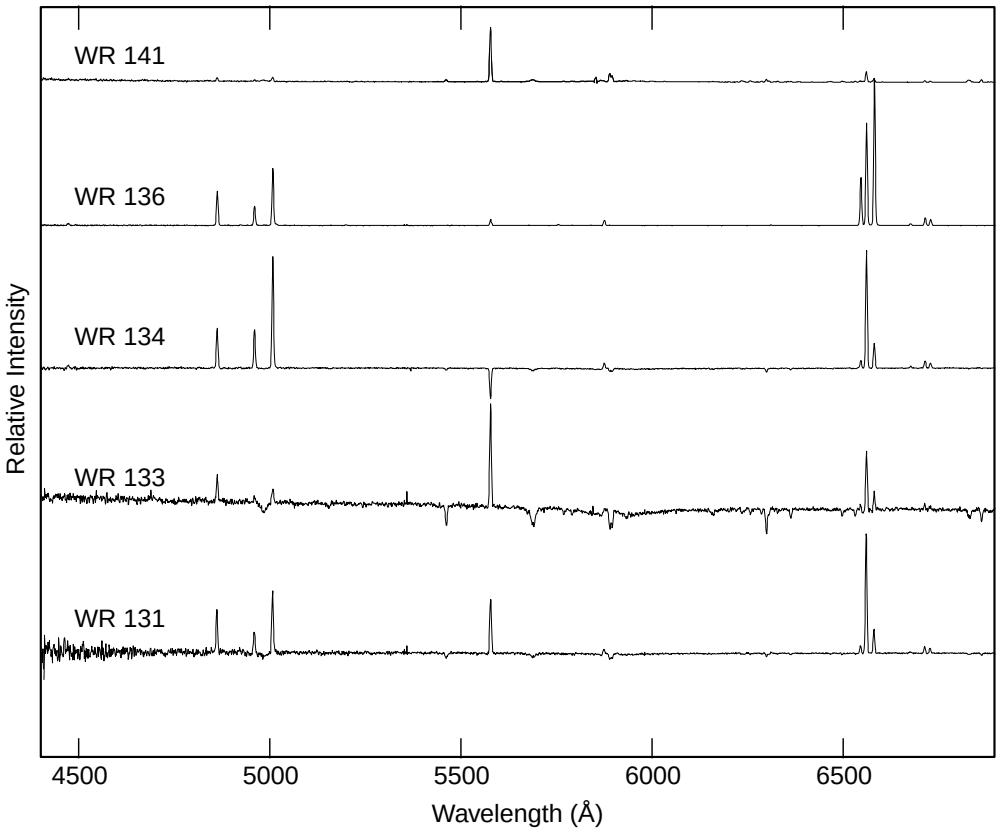

FIG. 2.—Dereddened spectra of WR nebulae, listed by the number of the central WR star. Note that the spectrum of WR 141 is of a different region than was used for photometry, as explained in § 2.2.

TABLE 1

PHYSICAL PARAMETERS OF WOLF-RAYET NEBULAE

Star	Alternate Designation	$E(B-V)$	Distance (kpc)	$L_{H\alpha}$ (ergs s^{-1})
WR 102...	LSS 4368	1.42	4.81 ± 0.46	$9.8 \pm 1.9 \times 10^{36}$
WR 113...	HD 168206	1.00	2.06 ± 0.12	$1.2 \pm 0.1 \times 10^{36}$
WR 116...	ST 1	1.28	3.15 ± 0.47	$1.4 \pm 0.4 \times 10^{36}$
WR 124...	209 BAC	1.15	4.46 ± 0.63	$8.9 \pm 2.5 \times 10^{35}$
WR 128...	HD 187282	0.59	4.01 ± 0.41	$2.8 \pm 0.6 \times 10^{35}$
WR 131...	MR 97	1.65	10.00 ± 0.90	$3.3 \pm 0.6 \times 10^{38}$
WR 133...	HD 190918	0.26	1.99 ± 0.16	$1.7 \pm 0.3 \times 10^{34}$
WR 134...	HD 191765	0.45	2.09 ± 0.09	$2.7 \pm 0.2 \times 10^{36}$
WR 136...	HD 192163	0.44	1.57 ± 0.11	$4.9 \pm 0.7 \times 10^{35}$
WR 141...	HD 193928	1.11	1.75 ± 0.18	$5.0 \pm 1.0 \times 10^{35}$

The derived reddening parameters are presented in Table 1. $E(B-V)$ values are generally consistent with the values derived by Hamann & Koesterke (1998) using the central WR stars. Spectra are shown in Figures 1 and 2, and logarithms of all key spectral lines (relative to Hα) are given in Table 2.

2.2. *Photometry*

Photometry of the nebulae associated with our selected WR stars[3] (WR 102, WR 113, WR 116, WR 124, WR 128, WR 131, WR 133, WR 134, WR 136, and WR 141) and of spectrophotometric standard stars selected from Massey et al. (1988) was obtained by K. D.-E. using the 0.9 m telescope at KPNO. Data were taken using the T2KA CCD. Our field of view was $23' \times 23'$, over 3 times the area of that used in the early survey by Miller & Chu (1993). The Hα filter was centered at 6573 Å, with an FWHM of 67 Å (including the [N II] emission lines at 6548 and 6583 Å) and a peak transmission of 80%. The off-band filter was centered at 6709 Å, with an FWHM of 71 Å and a peak transmission of 80% also.

Standard reductions were performed, including bias and flat-field corrections, and the off-band images were scaled and used to subtract out all stars from the Hα images. All of the observed nebulae are asymmetric to some degree, so custom apertures were required for each image. Using IRAF, we created custom polygonal apertures for each nebula to omit excessive empty sky flux, the detailed shape of which is dictated either by clear nebular boundaries or by contour lines for crowded fields. As shown in Figures A1 and A2 in the Appendix, some apertures are roughly circular while others are semicircular or quarter-circular.

While the exact three-dimensional structure of these nebulae is unknown, we presume that the exciting WR stars radiate in a spherically symmetric manner and that a Strömgren sphere of ionized gas would be visible if the hydrogen cloud was large and homogeneous (hence ionization bounded). Such a sphere would project a circular cross section on the plane of the sky. In the instance that ionized gas is only observed for a semicircular arc around the WR star, we assume that this is a result of either local nebular structure (producing density boundaries on this missing side) or obscuration by interstellar dust, and we multiply the ADU count by a factor of 2 to reconstruct the circular appearance of a spherically symmetric nebula as best as possible given our limited knowledge of the full geometry. In short, we multiplied the flux in semicircular apertures by 2.

In almost all cases, we placed our aperture around the nebula associated with the relevant WR star by the study of Miller & Chu (1993). However, we have chosen a different aperture location for the nebula surrounding WR 141. In their study, Miller & Chu's (1993) field of view was centered on the WR star itself and shows compact nebulosity to the northwest of the star (Fig. 1 of Miller & Chu 1993). Our reddening value computed to this nebulosity agrees to within 0.04 with the $E(B-V)$ value derived for the WR star itself by Hamann & Koesterke (1998), so the star is likely associated with the nebulosity to some degree. However, while this nebulosity appears somewhat spherically symmetric, the WR star lies on an outer edge of the nebula. The [O III] band image obtained by Miller & Chu (1993) shows a bright star located near the center of the nebula which may at first appear to be the ionization source instead; however, we identify this star to be variable star V* BI Cyg (IRAS 20194+3646), which is of spectral type M4. This M star cannot be the primary ionization source for the observed nebulosity, and therefore primary ionization is due to either the WR star or some other as yet undetermined early-type star.

Visible in our photometry, however, is a quarter-circle arc of nebulosity to the south of the WR star which is largely out of Miller & Chu's (1993) smaller field of view. This arc appears to be centered on WR 141, and we postulate that this nebulosity is part of an associated ring nebula photoionized by WR 141. Therefore, we place our photometric aperture around this partial ring nebula and avoid the confusing diffuse nebulosity to the north of the WR star. While the nebular spectrum has been obtained for the compact nebulosity to the northwest, we assume that this nebulosity has some association with the WR star and should at least be similar to the southern portion of the nebula.

Corrections to the photometry were made to account for the interstellar reddening and the presence of [N II] emission within the Hα bandpass. Reddening corrections were made based upon each value of $A_{H\alpha}$ derived from extinction values listed in Table 1. Relative contributions of [N II] and Hα emission were measured using the spectrum of each nebula (see Table 2), and the ADU count was fractionally adjusted accordingly to eliminate [N II] contribution.

3. NEBULAR PARAMETERS

3.1. *Distance Estimates*

Always a crux of any photometric study, accurate distances are essential to determining the luminosity of a source. To find the most accurate distance estimate for each WR nebula, we compiled independent measurements from a variety of sources which employed methods ranging from photometric distance moduli to Galactic kinematics models. Data were obtained from studies by Abbott et al. (1986), Conti & Vacca (1990), Crawford & Barlow (1991), Crowther, Hillier, & Smith (1995a), Crowther, Smith, & Hillier (1995b), Dufour (1989), Esteban & Rosado (1995), Massey, DeGioia-Eastwood, & Waterhouse (2001), van der

[3] In this paper we adopt the WR numbering system developed by van der Hucht et al. (1981); alternate designations are given in Table 1.

TABLE 2

SPECTRAL DATA OF WOLF-RAYET NEBULAE

Star	log [I(He II λ4686)/I(Hα)]	log [I(Hβ)/I(Hα)]	log [I([O III] λ5007)/I(Hα)]	log [I(He I λ5876)/I(Hα)]	log [I([O I] λ6300)/I(Hα)]	log [I([O I] λ6364)/I(Hα)]	log [I([N II] λ6548)/I(Hα)]	log [I([N II] λ6583)/I(Hα)]	log [I(He I λ6678)/I(Hα)]	log [I([S II] λ6717)/I(Hα)]	log [I([S II] λ6731)/I(Hα)]
WR 102...	−0.79	−0.49	0.25	−1.56	...	...	−0.88	−0.43	−2.06[a]	−0.91	−1.02
WR 113...	−2.05[a]	−0.48	−1.38	−1.83	...	...	−0.82	−0.32	−2.06	−1.03	−1.18
WR 116...	−1.08[a]	−0.47	...	−1.95[a]	−1.73	...	−0.85	−0.36	−2.09[a]	−0.84	−0.99
WR 124...	−2.27[a]	−0.48	−2.67	−2.38	...	...	−0.40	0.08	−3.15	−1.31	−1.27
WR 128...	−2.41[a]	−0.43	0.35	−1.17[a]	−0.25	−0.75	...	...	−1.37[a]	...	...
WR 131...	−0.07[a]	−0.48	−0.29	−1.29	...	...	−1.19	−0.71	−2.04	−1.27	−1.37
WR 133...	0.08[a]	−0.45	−0.57	−1.05[a]	...	...	...	−0.57	−1.42[a]	−1.27	...
WR 134...	−0.85[a]	−0.46	−0.03	−1.28	...	...	−1.22	−0.67	−1.83	−1.22	−1.35
WR 136...	−1.96[a]	−0.47	−0.25	−0.83	...	...	−0.34	0.15	−1.38	−1.12	−1.21
WR 141...	0.62[a]	−0.47	−0.36	−1.12[a]	−0.43	−0.92	...	−0.41	−1.60[a]	−0.81	−0.93

NOTE.—Logarithms of the spectral line intensities of dereddened spectra (assuming canonical $R = 3.1$). Dots denote where the given element line was not observed in the spectrum. Uncertainty in all logarithms is less than 0.15 dex; average uncertainty is estimated to be approximately 0.06 dex.

[a] Upper limit.

Hucht et al. (1988), and van der Hucht (2001). We obtain our distance estimates by computing the mean of the distances for each nebula determined in these studies and take as the uncertainty the standard deviation of the mean.

The assumed distances are presented in Table 1. Each distance estimate is the average of results from three to six independent studies.

One data point was discarded as a result of its location over 10 σ from the average of the other four data points. This estimate of $d = 9.37$ kpc for WR 128 (van der Hucht 2001) is based upon different assumptions concerning the binary nature of the star, and the implications of this greater distance will be discussed separately in a later section.

3.2. *Nebular Ionization Structure*

We consider the possible influence of shock excitation mechanisms on the net ionization state of the nebula. WR stars are well documented to possess extremely high mass-loss rates and strong stellar winds, and any substantial contribution from shock effects must be accounted for so that we do not overestimate the photoionizing emission from the WR star.

Photoionization and shock ionization possess signature patterns of element excitation, particularly in the [N II], [O III], and [S II] transitions. We analyzed our spectral data according to line ratios proposed by various authors:

1. log ([N II] λ6584/Hα) versus log ([O III] λ5007/Hβ) from Baldwin, Phillips, & Terlevich (1981) and Veilleux & Osterbrock (1987).
2. log ([S II] (λ6716 + λ6731)/Hα) versus log ([O III] λ5007/Hβ) from Veilleux & Osterbrock (1987).
3. log ([S II] (λ6717 + λ6731)/Hα) versus log ([N II] (λ6548 + λ6584)/Hα) from Levenson et al. (1995).
4. log (Hα/[S II] (λ6717 + λ6731)) versus [S II] λ6717/[S II] λ6731 from Esteban et al. (1992).

Figure 3 plots our data superimposed on the line ratio graph from Baldwin et al. (1981). Results from this graph are representative of the results given by all of our other line ratio plots, for which data are provided in Table 2.

Most WR nebulae were consistent with standard photoionization predictions in all comparisons. Individual nebulae are discussed below in greater detail and are referred to by the name of their central WR star.

3.2.1. *WR 102: LSS 4368*

WR 102 is somewhat inconsistent in line ratio comparisons as a result of [O III] and [N II] λ6584 excess. Treffers & Chu (1982) find that the nebula appears to include either part of an old supernova remnant or a large wind blown bubble but that the current excitation is more consistent with radiative ionization by the central WR star than with shock excitation mechanisms. Although the nebula likely contains abnormal metal abundances which produce the ionization inconsistencies on line ratio plots, it is reasonable to assume that exciting photoionization from WR 102 is the primary source of the observed nebular luminosity.

3.2.2. *WR 113: HD 168206*

WR 113 presents a clear case, consistent with photoionization on all line ratio comparisons. In addition, Miller & Chu (1993) find low [O III] emission as predicted for a

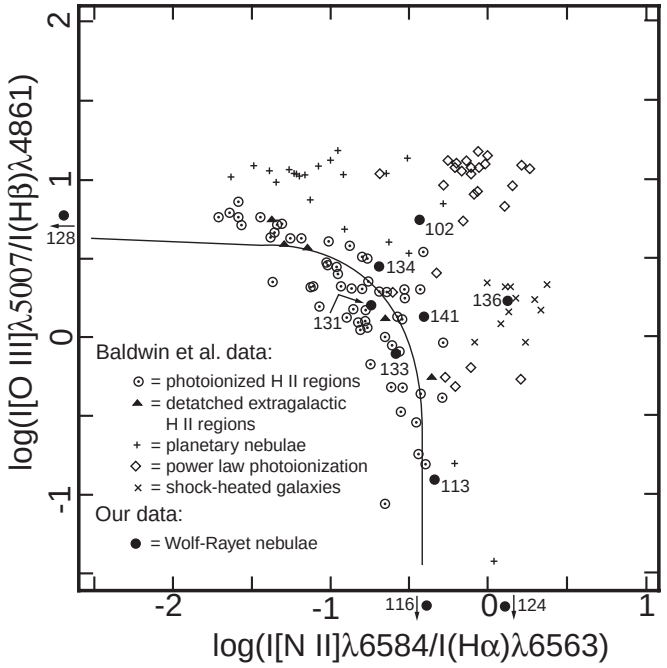

FIG. 3.—Spectral line intensity plot from Baldwin et al. (1981). Nebulae which plot outside graph boundaries have arrows pointing in the direction the nebula would plot (e.g., WR 116 is located at -0.36 on the horizontal axis but approaches $-\infty$ on the vertical axis as the [O III] line was either weak or absent in the nebular spectrum). The solid line represents simple photoionized H II region model predictions of Baldwin et al. (1981).

nebula photoionized by this late WN 9–type star, and Esteban & Rosado (1995) measure emission line ratios consistent with our results that lead them to conclude that photoionization is the primary excitation source of the nebula.

3.2.3. *WR 116: ST 1*

Like WR 113, WR 116 also has extremely low [O III] emission, consistent with photoionization by a late WN 8–type star (Miller & Chu 1993). When allowances are made for this [O III] intensity below usual for the average WR star, the nebular emission line ratios are consistent with photoionization on all plots. Esteban & Rosada (1995) concur from line ratios derived from their own spectra.

3.2.4. *WR 124: 209 BAC*

WR 124 appears somewhat inconsistent on line ratio plots, primarily because of an [O III] deficiency and an [N II] excess in the nebula, although available evidence indicates the presence of a WR ring nebula (Esteban et al. 1991; Crawford & Barlow 1991). As we lack a compelling argument suggesting significant shock ionization, we assume that photoionization dominates the excitation of the nebula as there appears no reason to believe otherwise.

3.2.5. *WR 128: HD 187282*

WR 128, however, does present a strong argument for significant shock contributions to the net ionization state. Major [N II] and [S II] deficiencies prevent us from making any of the relevant line ratio comparisons, and an extremely high [O I]/Hα ratio implies pronounced shock contributions. Miller & Chu (1993) and Esteban & Rosado (1995) both note the presence of [O III] filaments extending past the ionized H region, again indicative of shocks. Esteban &

Rosado (1995) also suggest that WR 128 may not be the primary ionization source for some parts of the nebula. However, as the nebula possesses clear semicircular symmetry centered closely on WR 128, we shall assume (with some reservations) that the WR star is the primary ionization source for the majority of the nebula, although strong shock-excited components are integral to the ionization structure.

3.2.6. *WR 131: MR 97*

WR 131 is consistent with photoionization in all comparisons, excepting a minor [S II] deficiency which may be abundance related. The nebula is superimposed on diffuse background nebulosity as noted by Chu & Treffers (1981), but accounting for this the primary nebula appears photoionized as the [O III] emission is only faint and diffuse (Miller & Chu 1993).

3.2.7. *WR 133: HD 190918*

WR 133 also appears inconsistent, agreeing well with photoionization predictions in some comparisons, yet appearing deficient in [S II]. It is believed that WR 133 is the ionization source for the nebula (Esteban & Rosado 1995), so we shall assume again that photoionization is the principle exciting mechanism in lack of any conclusive evidence to the contrary.

3.2.8. *WR 134: HD 191765*

A somewhat unique situation arises in the case of WR 134, where our comparisons and research by Miller & Chu (1993), Esteban & Rosado (1995), and Gervais & St-Louis (1999) indicate that the northwest sector of the semicircular ring nebula is mainly shock excited while the southwest sector is predominantly photoionized. Such clear divisions within a nebula are highly unusual and present unique opportunities for detailed study of shock ionization effects. However, in this analysis we wish to confine our study as closely as possible to photoionized nebulae, and so we construct a special aperture over only the southwest quadrant of the nebula, thereby largely ignoring contributions from shock effects.

3.2.9. *WR 136: HD 192163*

By far the most impressive WR nebula, that surrounding WR 136 is also the only nebula in our study to merit an NGC listing (NGC 6888). Both our plots and current literature, e.g., Miller & Chu (1993) and Dufour (1989), show that the nebula appears to contain both photoionization and shock ionization sources. Moore, Hester, & Scowen (2000) have performed an extensive study of this source, and we therefore proceed with our analysis of this nebula in order to compare results in § 5.

3.2.10. *WR 141: HD 193928*

While Miller & Chu (1993) list WR 141 only as embedded "in nebulosity," we believe that we have located a partial ring nebula for the star as explained in § 2.2. Spectroscopy obtained of the old nebulosity (as detailed in § 2.2) is compatible with photoionization in all line ratio comparisons.

3.3. Hα *Luminosity*

The Hα luminosity of each nebula was calculated from the flux in each aperture using standard stars selected from Massey et al. (1988) and corrected for reddening, [N II] contamination, and aperture geometry as previously described. Measurements were corrected to zero air mass and converted to fluxes at the telescope in ergs s^{-1} cm^{-2} using the Vega calibration of Hayes & Latham (1975) as referenced by Massey et al. (1988). Using the distances derived in § 3.1, we converted these fluxes to luminosities, presented in Table 1. Uncertainties quoted in this table include contributions from photon noise, distance uncertainty, and uncertainties in the spectrophotometric calibration.

4. ANALYSIS OF IONIZING FLUXES

4.1. Q_0: H-*Ionizing Flux*

4.1.1. *Notes on the Lower Bound*

In an ideal situation, the hydrogen clouds surrounding the studied WR stars would be large and optically thick enough to completely absorb all ionizing photons from the central star (ionization bounded). As well illustrated by NGC 6888, however, real nebulae are not generally homogenous agglomerations of optically thick gas but instead are patchy and often composed of clumps of gas of varying optical depth distributed throughout a thin diffuse background medium. As a result, some ionizing photons are bound to escape the nebula as a result of optically thin "holes" in the nebular structure (e.g., Oey et al. 2000).

Simplistically, assuming spherically symmetric radiation from the WR star, we can analogously describe the volume integral of Lyman continuum absorption over the entire nebula as a surface integral over an optically thick "Strömgren Wiffle ball" shell of radius r_0 containing holes of opacity zero. We can then describe the effective surface filling factor (fractional ionization) of this hole-riddled shell for absorbing Lyman continuum radiation by a simple geometric factor χ_0 with value between 0 and 1, defined in terms of the number of H-ionizing photons Q_0 by

$$Q_0(\text{observed}) = \chi_0\, Q_0(\text{actual}) \,. \tag{1}$$

Corresponding factors χ_1 and χ_2 for He^0- and He^+-ionizing radiation, respectively, are defined in a similar manner.

The observed luminosity of the nebula is certainly less than that of a corresponding Strömgren sphere of gas. Lacking almost any knowledge concerning the actual geometry of the nebula, we can only estimate the ionizing flux required to produce the observed nebular Hα luminosity. Therefore, our calculated ionizing fluxes serve as lower bounds to the actual ionizing fluxes of the stars, and future studies employing a modified Zanstra method would require some knowledge of the geometrical factor χ_0 in order to reconstruct the actual ionizing fluxes.

4.1.2. *Procedure*

As derived in Osterbrock (1974), we use the observed nebular Hα luminosity to calculate the total flux of photons from the central WR star with energy greater than that required to ionize hydrogen ($\nu \geq 3.29 \times 10^{15}$ Hz). In local thermodynamic equilibrium (LTE), ionizations are balanced by e^- recaptures per unit time, so

$$\int_{\nu_0}^{\infty} \frac{L_\nu}{h\nu} d\nu = Q_0 = \int_0^{r_0} N_p\, N_e\, \alpha_B(H^0, T) dV \,, \tag{2}$$

where the right-hand side of the equation is an integral over the entire volume of the ionized region. N_p is the proton number density, N_e is the electron number density, $\alpha_B(H^0, T)$ is a recombination coefficient dependent upon the density of neutral hydrogen atoms and temperature of the nebula, and Q_0 is the total number of H-ionizing photons emitted per second.

Based on recombinations throughout the nebula, the luminosity of the nebula can be described by

$$L_{\mathrm{H}\alpha} = h\nu_{\mathrm{H}\alpha} \int_0^{r_0} N_p N_e \alpha_{\mathrm{H}\alpha}^{\mathrm{eff}}(H^0, T) dV \ , \quad (3)$$

where $\alpha_{\mathrm{H}\alpha}^{\mathrm{eff}}(H^0, T)$ is a wavelength-specific recombination coefficient dependent upon neutral hydrogen density and temperature.

Dividing equation (3) by equation (2) and taking each α out of its integral, as the recombination coefficients are approximately constant across the volume of the nebula, we obtain

$$\frac{L_{\mathrm{H}\alpha}}{Q_0} = \frac{h\nu_{\mathrm{H}\alpha}\alpha_{\mathrm{H}\alpha}^{\mathrm{eff}} \int_0^{r_0} N_p N_e dV}{\alpha_B \int_0^{r_0} N_p N_e dV} \ . \quad (4)$$

Canceling the integrals and rearranging, we conclude that

$$Q_0 = \frac{\alpha_B L_{\mathrm{H}\alpha}}{h\nu_{\mathrm{H}\alpha}\alpha_{\mathrm{H}\alpha}^{\mathrm{eff}}} \ . \quad (5)$$

The ratio $\alpha_B/\alpha_{\mathrm{H}\alpha}^{\mathrm{eff}}$ depends only weakly on the temperature T of the nebula and the electron density N_e. With reasonable estimates of $T = 10{,}000$ K and $N_e = 10^3$ cm^{-3}, under case B recombination Table 4.4 of Osterbrock (1974) gives

$$\alpha_{\mathrm{H}\alpha}^{\mathrm{eff}} = \frac{j_{\mathrm{H}\alpha}}{j_{\mathrm{H}\beta}} \alpha_{\mathrm{H}\beta}^{\mathrm{eff}} = 8.70 \times 10^{-14} \ \mathrm{cm}^3 \ \mathrm{s}^{-1} \ . \quad (6)$$

Using these estimates for temperature and N_e, from Table 2.1 of Osterbrock (1974) we obtain

$$\alpha_B = 2.60 \times 10^{-13} \ \mathrm{cm}^3 \ \mathrm{s}^{-1} \ . \quad (7)$$

If we were instead to assume that $N_e \approx 10^2$ cm^{-3} as has been used in many studies, then the ratio $\alpha_B/\alpha_{\mathrm{H}\alpha}^{\mathrm{eff}}$ increases by less than 1%. Thus, we use our measured $L_{\mathrm{H}\alpha}$ to calculate a lower bound to the total photon emission of the star at energies high enough to ionize neutral hydrogen. Table 3 gives the logarithm of the number of ionizing photons per second (log Q_0) for each WR star; log Q_0 is graphed versus spectral type in Figure 4.

Figure 4 presents certain notable features. First, WR 131 (WN 7) appears to emit over 2 orders of magnitude more H-ionizing flux than all of the other stars. This could be due in part to its anomalous distance of 10 kpc, although arbitrarily reassigning it a distance of 4 kpc only decreases log Q_0 to 49.7. Despite precautions, diffuse background emission may have been counted within our aperture, χ_0 may prove much higher than normal for this nebula, contamination from other stars may be significant, or the star itself may be abnormally bright. Alternatively, we may have assumed too high a reddening for WR 131, as the lower $E(B-V)$ value of Hamann & Koesterke (1998) would produce a more reasonable lower bound for Q_0. Likely, a combination of these effects is in evidence.

TABLE 3

LOWER BOUNDS TO THE IONIZING RADIATION OF WOLF-RAYET STARS

Star	Spectral Type	log Q_0	log Q_1	log Q_2
WR 102...	WO 1	48.98 ± 0.08	47.77 ± 0.16	48.19 ± 0.14
WR 113...	WN 9	48.08 ± 0.05	46.84 ± 0.07	46.02 ± 0.05[a]
WR 116...	WN 8	48.13 ± 0.13	46.52 ± 0.13[a]	46.74 ± 0.13[a]
WR 124...	WN 8	47.94 ± 0.12	45.90 ± 0.15	45.34 ± 0.12[a]
WR 128...	WN 4	47.44 ± 0.09	46.60 ± 0.09[a]	46.50 ± 0.09[a]
WR 131...	WN 7	50.51 ± 0.08	49.56 ± 0.14	49.26 ± 0.08[a]
WR 133...	WN 4.5	46.24 ± 0.07	45.52 ± 0.07[a]	45.20 ± 0.07[a]
WR 134...	WN 6	48.42 ± 0.04	47.48 ± 0.06	46.40 ± 0.04[a]
WR 136...	WN 6	47.69 ± 0.06	46.76 ± 0.08	45.42 ± 0.06[a]
WR 141...	WN 6	47.69 ± 0.09	46.91 ± 0.09[a]	46.73 ± 0.09[a]

[a] Upper limit.

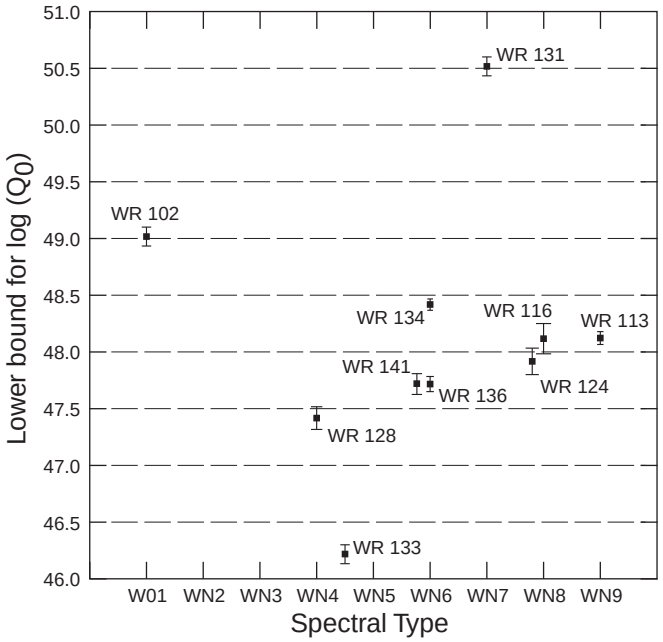

FIG. 4.—H-ionizing flux data from Table 3; note that WR 102 is a "WO 1"–type star while all other stars are WN type.

In addition, it appears possible that early "WO"-type stars may emit more H-ionizing flux than WN-type stars, as indicated by the greater Q_0 of the WO 1 star WR 102 compared to all WN class stars except the abnormal WR 131. This conclusion is based solely upon the measurement of one WO class star, however, and is not definitive.

WR 133 (WN 4.5) presents the opposite complication: it appears to emit less H-ionizing flux than the other stars. The most likely explanation for this is that χ_0 for this nebula is abnormally small compared to the other nebulae.

Finally, while the geometric factor χ_0 should in theory vary considerably from nebula to nebula depending upon local gas density and distribution, the remaining data points appear relatively consistent between a range of roughly log $Q_0 = 47.5$ and 48.5. If we assume van der Hucht's (2001) distance to WR 128 of $d = 9.37$ kpc, then WR 128 rises from log $Q_0 = 47.4$ to a value of 48.2, in excellent accord with the other data. This rough correlation of data about log $Q_0 = 48$ suggests not only that the average value of χ_0 is relatively consistent in all nebulae, but also that the luminosity of mid- to late WN spectral types is only loosely, if indeed at all, dependent on spectral type.

4.2. Q_1 and Q_2: He-*Ionizing Fluxes*

4.2.1. *Notes on the Lower Bound and Upper Limits*

Using our spectroscopic data, we consider the hardness of the ionizing spectrum by calculating bounds for the He^0- and He^+-ionizing fluxes. We estimate the nebular luminosity at the He I transition lines $\lambda\lambda$5876 and 6678 by multiplying $L_{\mathrm{H}\alpha}$ by the line intensity ratios $I_{\lambda 5876(\mathrm{He\ I})}/I_{\lambda 6563(\mathrm{H}\alpha)}$ and $I_{\lambda 6678(\mathrm{He\ I})}/I_{\lambda 6563(\mathrm{H}\alpha)}$, respectively. In the event that He I or He II lines were not visible in our spectra, we estimated the minimum intensity required for these lines to stand out

by a 3 σ deviation from the noise at an average FWHM of 4.2 Å. In the instances where we could not measure the observed luminosity at one of these wavelengths, we used this upper limit instead. He/Hα ratios are given in Table 2, and upper limit estimates are noted. To keep terminology as clear as possible, we shall always refer to this 3 σ estimate as an upper limit, while the estimate of the ionizing fluxes shall always be referred to as a lower bound.

We must also consider the effect of low-opacity clouds and density-bounded regions on these estimates. Osterbrock (1974) finds that for stars of temperature $T_* \geq$ 40,000 K the H- and He^0-ionizing regions of the surrounding nebulae are coincident, while temperatures of $T_* \geq$ 100,000 K are required for the He^+-ionizing region to also become coincident with the H-ionizing region. Despite the difficulty in constraining T_* precisely as a result of atmospheric effects, it is reasonably safe to assume that WR stars will behave somewhat like stars in this 60,000 K range as observational estimates for the effective temperature of WR stars usually lie in the range $T_* \approx$ 50,000–90,000 K (Schmutz, Leitherer, & Gruenwald 1992). Therefore, we believe that it is safe to assume in our nebulae that H- and He^0-ionizing regions are coincident while He^+-ionizing regions are somewhat smaller.

At the outer boundary of the nebula r_0, variable opacity and density produce $\chi_0 < 1$, and it is probable that $\chi_2 > \chi_0$ as the He^+-ionizing flux does not penetrate as far into the surrounding gas and therefore has a higher percentage of photons absorbed within the nebula. As the H- and He^0-ionizing regions are coincident, the H- and He^0-ionizing radiation should experience similar absorption in any given region of the nebula. Across the nebula then, we should expect $\chi_1 \approx \chi_0$. In conclusion, we assume that

$$\chi_2 > \chi_1 \approx \chi_0 \, . \tag{8}$$

Effectively, equation (8) means that if the line intensity ratio is measured, our method will determine a lower bound for Q_1. If an upper limit to the ratio is estimated, our method will determine the maximum possible lower bound for Q_1. Q_2 can be treated identically.

4.2.2. He^0-*Ionizing Flux*

Analogously to the derivation of the number of H-ionizing photons Q_0 in § 4.1.2, the number of He^0-ionizing photons can be written in equivalent ways using the two separate He I emission lines $\lambda\lambda$5876 and 6678:

$$Q_1 = \frac{\alpha_B L_{\lambda 5876}}{h\nu_{\lambda 5876}\, \alpha^{\rm eff}_{\lambda 5876}} \tag{9}$$

and

$$Q_1 = \frac{\alpha_B L_{\lambda 6678}}{h\nu_{\lambda 6678}\, \alpha^{\rm eff}_{\lambda 6678}} \, . \tag{10}$$

Using spectral line ratios to determine $L_{\lambda 5876}$ and $L_{\lambda 6678}$, we use these two equations to provide independent estimates of Q_1, which we compare to gauge the internal consistency of our method. In all cases in which actual He I lines were measured, the two estimates are consistent to within the uncertainty given in Table 3. In addition, for WR 102, which presented a visible λ5876 but required an upper limit estimate for λ6678, the upper limit estimate was greater than the value measured using the visible spectral line. All other upper limit estimates proved reasonably consistent to within less than half an order of magnitude, with λ5876 consistently providing the lower of the two estimates. Our data appear internally consistent to within uncertainty, and we present the data from λ5876 as this stronger spectral line provides a tighter upper limit constraint on the actual values. In Figure 5 we plot the calculated lower bound estimates for Q_1 versus spectral type, and Table 3 contains a detailed list of these values.

WR 131 and WR 133 exhibit the same abnormally high and low Q_1 behavior, respectively, in Figure 5 as they did in Figure 4, and the remaining data show considerably more scatter. While potentially due in part to the dependence of our 3 σ method of estimating upper limits on the noise level in a particular spectrum, this could also be a sign of increasing scatter in χ_1. The available data still do not suggest any general trend, further casting into doubt any significant dependence of luminosity on spectral type.

4.2.3. He^+-*Ionizing Flux*

Again following the same derivation used for H- and He^0-ionizing fluxes, we determine

$$Q_2 = \frac{\alpha_B L_{\lambda 4686}}{h\nu_{\lambda 4686}\, \alpha^{\rm eff}_{\lambda 4686}} \, . \tag{11}$$

In this case, only WR 102 exhibits a measurable He II emission line, and 3 σ upper limit estimates are given for all other stars.

Figure 6 graphs the calculated maximum lower bound estimates for Q_2 versus spectral type, and a more detailed list of these values is included in Table 3. Strangely, Table 3 shows that log $Q_2 >$ log Q_1 by almost 0.4 dex for WR 102. This statement is impossible as $Q_2 \subseteq Q_1$ (He^+-ionizing flux is a subset of the He^0-ionizing flux), and we conclude that some other factor must be causing the observed excess. In lack of a similar spectral class to compare to, however, we cannot draw any concrete conclusions. A similar case occurs for WR 116, although in this instance estimates for both Q_1 and Q_2 are upper limits calculated using our 3 σ

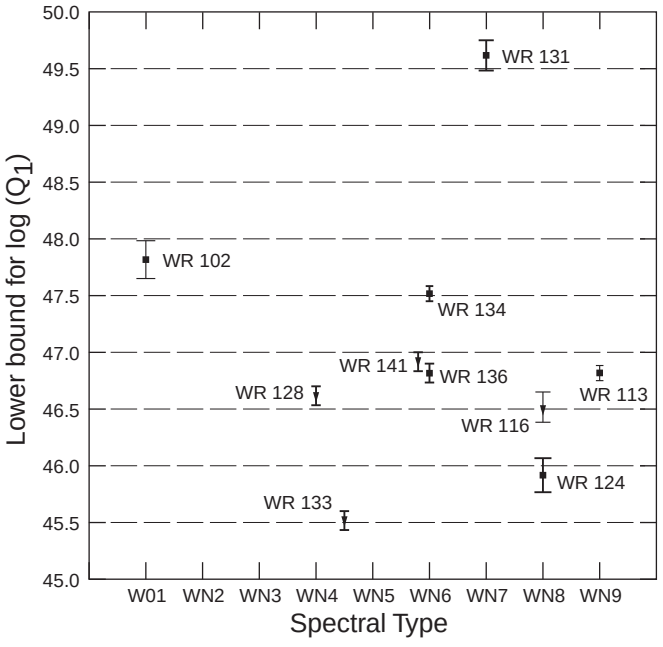

FIG. 5.—He^0-ionizing flux data are as described in Fig. 4. The filled squares denote a measured value, while the downward arrows denote an upper limit computed using a 3 σ estimate.

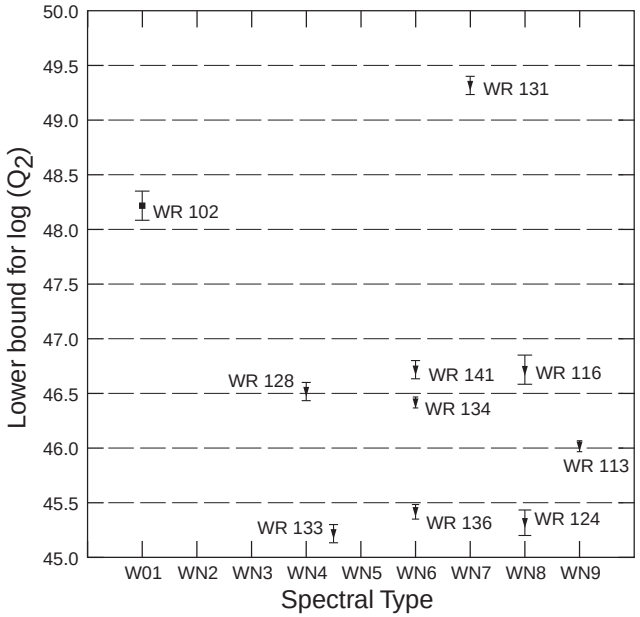

FIG. 6.—He^+-ionizing flux data are as described in Fig. 4; symbols are the same as in Fig. 5.

method, and discrepancies can be attributed to variations in the noise level at different locations in our spectrum.

Figure 6 shows the same abnormal behavior of WR 131 and WR 102 as in Figures 4 and 5 and also exhibits considerable scatter within other data points, likely resulting from effects of noise fluctuation on our 3 σ upper limit estimate and varying χ_2. However, there still does not appear to be any trend with spectral type that we can discern from our upper limit data.

5. DISCUSSION

The results in Table 3 are consistent with those from the relatively few previous studies. The result for WR 136 ($\log Q_0 \gtrsim 47.69 \pm 0.06$) agrees well with the study of Marston & Meaburn (1988), who determine $\log Q_0 = 47.6$ using a modified Zanstra method similar to our own.

Moore et al. (2000) discuss at length the discrepancy between Marston & Meaburn's (1988) value and their own determination of $\log Q_0 = 49.3$, which provided the best fit for their atmospheric models using the nebular modeling program CLOUDY (Ferland 1996). Their conclusion is largely identical to our discussion in § 4.1.1, that the Zanstra method underestimates the total flux from the star because of clumping in the nebula. Comparing Marston & Meaburn's (1988) value of $\log Q_0 = 47.6$ to their best-fit value of $\log Q_0 = 49.3$, Moore et al. (2000) determine that only about 2% of the H-ionizing photons produced by WR 136 are processed within the nebula. Equivalently, this processing percentage is an estimate of the geometrical factor χ_0, suggesting $\chi_0 \approx 0.02$. The close agreement of our results with those of Marston & Meaburn (1988) and the fairly consistent values of $\log Q_0 \gtrsim 48.0$ in Figure 4 suggest that $\chi_0 \approx 0.02$ may be a reasonable estimate for most of the WN stars in our sample.

Crowther et al. (1999) model the ionizing flux of WR 124 using CMFGEN (Hillier 1987, 1990; Hillier & Miller 1998) and the Sobolev approximation code ISA-wind (described by de Koter, Schmutz, & Lamers 1993; de Koter, Heap, & Hubeny 1997). CMFGEN and ISA-wind each predict roughly $\log Q_0 = 49$ for both line-blanketed and non-blanketed models (consistent with the study by Moore et al. 2000 and the estimated χ_0 obtained thereof), and the non-blanketed CMFGEN and blanketed ISA-wind models each predict $\log Q_1 \approx 48$ while blanketed CMFGEN predicts $\log Q_1 \approx 44$. Figure 5 shows $\log Q_1 \gtrsim 46.0$, which is clearly inconsistent with the blanketed CMFGEN model in this case. However, L. Smith & P. A. Crowther (2001, private communication) have recently made blanketed CMFGEN models of WR 40 (HD 96548, WN 8) and WR 6 (HD 50896, WN 5). For WR 40 they used a higher temperature (determined by Herald, Hillier, & Schulte-Ladbeck 2001) than was used in their earlier WR 124 model and predicted $\log Q_0$ and $\log Q_1$ of about 49.7 and 48.8, respectively. Their blanketed model for WR 6 predicted $\log Q_0$ and $\log Q_1$ equal to 49.3 and 49.0, respectively. Clearly, our data are consistent with blanketed CMFGEN predictions in some, although not all, cases. Therefore, further comparisons are required to more generally constrain the model results. Model predictions for the ionizing fluxes are listed in Table 4; predictions for $\log Q_2$ (where available) are included but cannot be used to decide between models as we have only been able to determine upper limits to the lower bound for $\log Q_2$.

The spectrum of WN stars appears fairly hard, with nonnegligible flux above the He^0 edge at 504 Å but very little flux above the He^+ edge at 228 Å. Figure 5 exhibits lower bounds of Q_1 ranging from about 10^{46} to 10^{47} s^{-1}. Assuming again that $\chi_1 \approx \chi_0$, the number of He^0-ionizing photons appears about 1–2 orders of magnitude less than the number of H-ionizing photons, which clusters around $Q_0 \gtrsim 10^{48}$ s^{-1}. Figure 6 shows the lower bounds of Q_2 ranging from 10^{45} to $10^{46.5}$ s^{-1}, approximately another order of magnitude less than estimates of Q_1 and therefore 2–3 orders of magnitude less than the lower bound estimate for Q_0. However, as $\chi_2 > \chi_0$ more He^+-ionizing photons may be absorbed in the nebula than if $\chi_2 \approx \chi_0$, and combined with our 3 σ upper limit estimate it is therefore unlikely that $Q_2 > 10^{46.5}$ s^{-1} and probable that it is somewhat less.

TABLE 4

MODEL PREDICTIONS OF THE IONIZING FLUX

Model	Star	Line Blanketing	$\log Q_0$	$\log Q_1$	$\log Q_2$	Reference
CMFGEN.....	WR 124	Yes	49.05	43.88	...	1
CMFGEN.....	WR 124	No	49.05	48.19	...	1
CMFGEN.....	WR 6	Yes	49.3	49.0	40.5	2
CMFGEN.....	WR 40	Yes	49.65	48.79	39.08	2
ISA-wind	WR 124	Yes	49.00	47.91	...	1

REFERENCES.—(1) Crowther et al. 1999. (2) L. J. Smith & P. A. Crowther 2001, private communication.

The early "WO"-type star WR 102 appears to have a considerably harder far-UV spectrum (roughly 10% of the H-ionizing flux also energetic enough to ionize He^+) than do WN stars (at most 1% of the H-ionizing flux energetic enough to also ionize He^+). He II lines are not visible in any nebulae associated with WN class stars, and the 3 σ upper limit estimate of He^+-ionizing flux contributing from 0.1% to 1% of the total H-ionizing flux may indeed prove a considerable overestimate. The non-LTE predictions of Schmutz et al. (1992) concur with this result, expecting negligible flux shortward of 228 Å. While this behavior may be representative of the "WO" type as a whole, further study is required to confirm the possibility.

Oey & Kennicutt (1997) project from a private communication with P. A. Crowther that $\log Q_0 = 49$ is a reasonable estimate for the ionizing emission of WNE stars, consistent with our lower bound estimate of $\log Q_0 \gtrsim 48$. However, absolute empirical determinations of the ionizing fluxes of WR stars and tighter constraints on stellar atmosphere models await primarily a knowledge of the geometry factor χ and its value for various wavelengths of emission. Results appear to suggest that the H-ionizing flux is independent of WN spectral type and that χ may not vary greatly from nebula to nebula (possibly $\chi_0 \approx 0.02$). If this proves to be the case, then we should expect approximately $49 \leq \log Q_0 \leq 50$ for WN class stars.

The authors are grateful to the NSF for grant AST-9988007 funding the REU program at NAU. D. R. L. would also like to thank K. A. van der Hucht for clarification regarding distance estimates for WR 128 in the Seventh Catalogue of Galactic Wolf-Rayet Stars, Phil Massey and Sally Oey of Lowell Observatory for helpful comments and feedback on preliminary drafts of this paper, and Linda Smith and Paul Crowther for making available their latest prepublication models.

APPENDIX

Star-subtracted Hα photometry is shown in Figures A1 and A2.

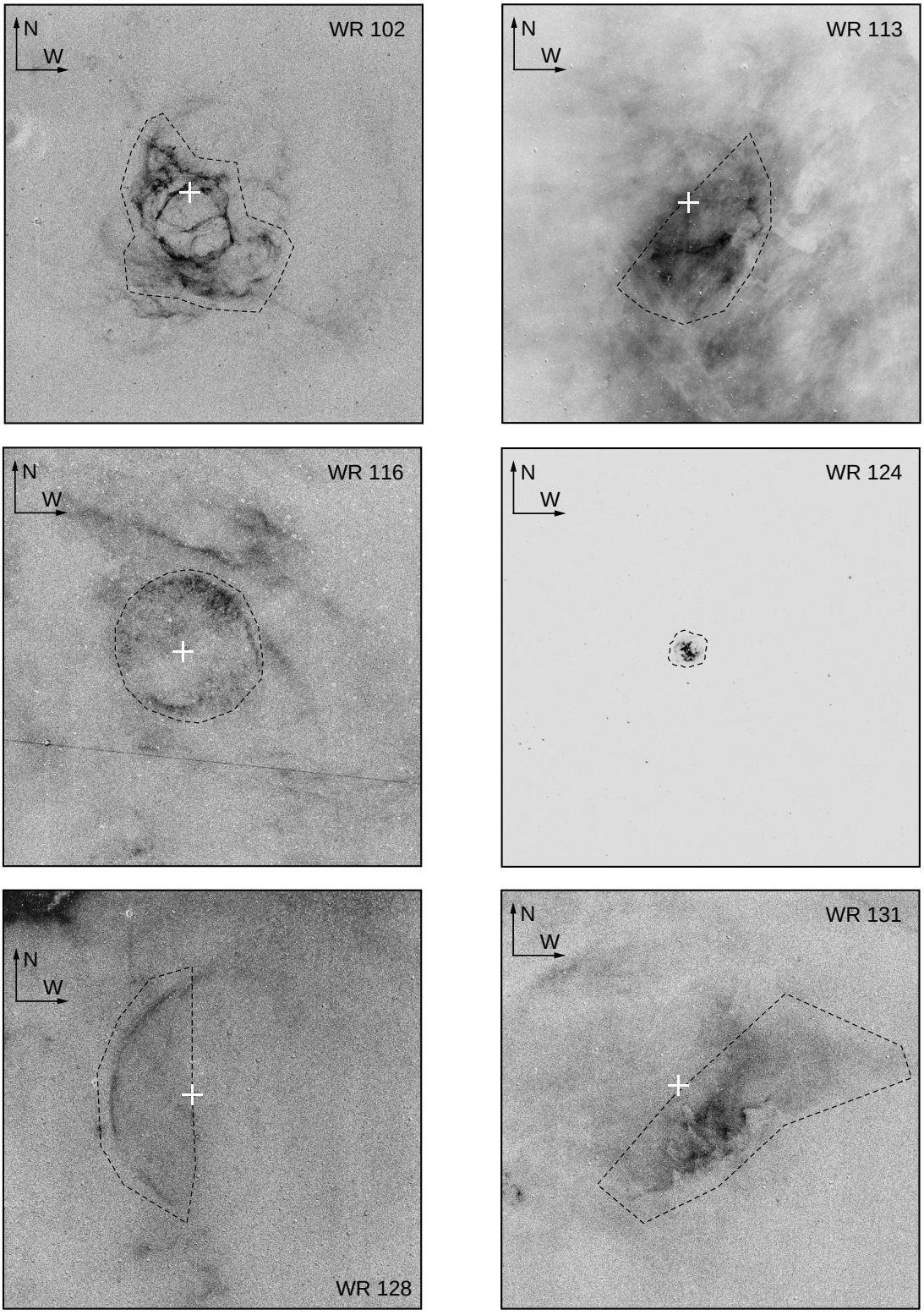

FIG. A1.—Star-subtracted Hα photometry; field of view is 23′ × 23′, plus signs denote the location of the central WR star, and a dashed line denotes the placement of the custom aperture.

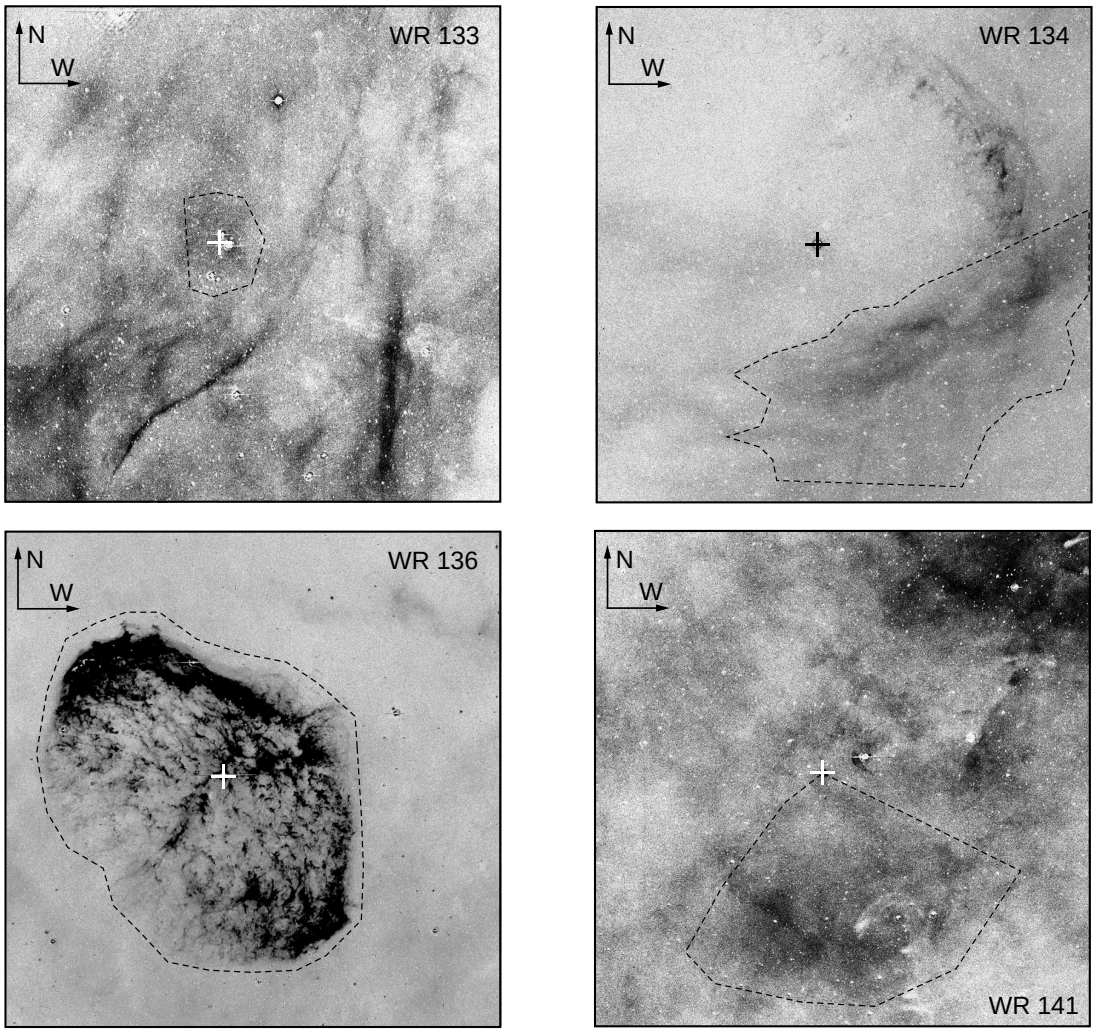

FIG. A2.—Same as Fig. A1

REFERENCES

Abbott, D. C., Torres, A. V., Bieging, J. H., & Churchwell, E. 1986, ApJ, 303, 239
Baldwin, J. A., Phillips, M. M., & Terlevich, R. 1981, PASP, 93, 5
Chu, Y. H., & Treffers, R. R. 1981, ApJ, 250, 615
Conti, P. S. 2000, PASP, 112, 1413
Conti, P. S., & Vacca, W. D. 1990, AJ, 100, 431
Crawford, I. A., & Barlow, M. J. 1991, A&A, 249, 518
Crowther, P. A., Hillier, D. J., & Smith, L. J. 1995a, A&A, 293, 403
Crowther, P. A., Pasquali, A., de Marco, O., Schmutz, W., Hillier, D. J., & de Koter, A. 1999, A&A, 350, 1007
Crowther, P. A., Smith, L. J., & Hillier, D. J. 1995b, A&A, 302, 457
de Koter, A., Heap, S. R., & Hubeny, I. 1997, ApJ, 477, 792
de Koter, A., Schmutz, W., & Lamers, H. J. G. L. M. 1993, A&A, 277, 561
Dufour, R. J. 1989, Rev. Mexicana Astron. Astrofis., 18, 87
Esteban, C., & Rosado, M. 1995, A&A, 304, 491
Esteban, C., Vilchez, J. M., Manchado, A., & Smith, L. J. 1991, A&A, 244, 205
Esteban, C., Vilchez, J. M., Smith, L. J., & Clegg, R. E. S. 1992, A&A, 259, 629
Ferland, G. J. 1996, Hazy, a Brief Introduction to Cloudy 90, Univ. Kentucky, Phys. Dept. Internal Rep.
Gervais, S., & St-Louis, N. 1999, AJ, 118, 2394
Hamann, W. R., & Koesterke, L. 1998, A&A, 333, 251
Hayes, D. S., & Latham, D. W. 1975, ApJ, 197, 593
Herald, J. E., Hillier, D. J., & Schulte-Ladbeck, R. E. 2001, ApJ, 548, 932
Hillier, D. J. 1987, ApJS, 63, 947
Hillier, D. J. 1990, A&A, 231, 111
Hillier, D. J., & Miller, D. L. 1998, ApJ, 496, 407
Levenson, N. A., Kirshner, R. P., Blair, W. P., & Winkler, P. F. 1995, AJ, 110, 739
Marston, A. P., & Meaburn, J. 1988, MNRAS, 235, 391
Massey, P., DeGioia-Eastwood, K., & Waterhouse, E. 2001, AJ, 121, 1050
Massey, P., Strobel, K., Barnes, J. V., & Anderson, E. 1988, ApJ, 328, 315
Miller, G. J., & Chu, Y. H. 1993, ApJS, 85, 137
Moore, D., Hester, J. J., & Scowen, P. A. 2000, AJ, 119, 2991
Oey, M. S., Dopita, M. A., Shields, J. C., & Smith, R. C. 2000, ApJS, 128, 511
Oey, M. S., & Kennicutt, R. C., Jr. 1997, MNRAS, 291, 827
Osterbrock, D. E. 1974, Astrophysics of Gaseous Nebulae (San Francisco: Freeman)
Savage, B. D., & Mathis, J. S. 1979, ARA&A, 17, 73
Schmutz, W., Leitherer, C., & Gruenwald, R. 1992, PASP, 104, 1164
Smith, L. J. 1995, in IAU Symp. 163, Wolf-Rayet Stars: Binaries, Colliding Winds, Evolution, ed. K. A. van der Hucht & P. M. Williams (Dordrecht: Kluwer), 24
Treffers, R. R., & Chu, Y. H. 1982, ApJ, 254, 132
van der Hucht, K. A. 2001, NewA Rev., 45, 135
van der Hucht, K. A., Conti, P. S., Lundstrom, I., & Stenholm, B. 1981, Space Sci. Rev., 28, 227
van der Hucht, K. A., Hidayat, B., Admiranto, A. G., Supelli, K. R., & Doom, C. 1988, A&A, 199, 217
Veilleux, S., & Osterbrock, D. E. 1987, ApJS, 63, 295